Layered Open Pore Poly(L-lactic acid) Nanomorphology

Xia Liao,[†] A. Victoria Nawaby,*[,†] Pamela Whitfield,[†] Michael Day,[†] Michel Champagne,[‡] and Johanne Denault[‡]

Institute for Chemical Process and Environmental Technology, National Research Council of Canada, Ottawa, Ontario, K1A 0R6 Canada, and Industrial Materials Institute, National Research Council of Canada, Boucherville, Quebec, J4B 6Y4 Canada

Received July 27, 2006; Revised Manuscript Received September 8, 2006

This paper reports on specific open and interconnected CO_2 foams of poly(L-lactic acid). The effect of varying gas concentration and hence physical changes induced by CO_2 has been investigated and thus used to generate specific structures. The developed morphologies have a skin core structure with larger pores in the core and open and interconnected smaller pores in the skin.

Introduction

The design of templates seeded with biological cells from a tissue bank or a patient's own system for the purpose of tissue regeneration or repair is an area of active research. Numerous research activities are underway to create biomimetic templates with a wide range of geometries for biological and medical applications.[1] An ideal bioresorbable scaffold provides a substrate for cell growth while maintaining cell activity, leading to a self-supporting structure. The subsequent degradation of the scaffold itself must not cause harm to the growing cells and surrounding tissues.[2]

Lack of suitable and ideal tissue for transplantation is a driving factor for the tissue engineering field to find elegant solutions. Depending upon the biological tissue and cell's needed, processing techniques are being developed and scaffolds with different functionalities are produced. Areas of success include development of multichannel, biodegradable scaffolds for the promotion of spinal cord axon regeneration using a solution of poly(D,L-lactide-*co*-glycolic acid) in dichloromethane and a specifically designed Teflon mould.[3] In addition, poly-(D,L-lactide-co-glycolic acid) (PLGA) processed with a combination of high-pressure carbon dioxide (CO_2) and a salt (NaCl) leaching technique has produced a highly interconnected porous structure.[4] Other reported studies on generating porous structures with open and interconnected morphologies for biomedical applications include emulsion freeze drying,[5] phase separation,[6,7] fiber forming,[8] and 3D printing.[9] Nevertheless, a major draw back of the reported studies is the use of organic solvents during processing and/or using elevated temperatures with the possibility of the denaturing of active molecules in the matrix.

Use of only CO_2 gas as a processing aid provides the possibility of generating scaffolds from biopolymers without the use of harmful organics or a high-temperature process. Creation of scaffolds in the case of PLGA (85/15)−CO_2 system with some degree of success was demonstrated.[2] The resultant scaffolds produced by CO_2 at room temperature and pressures up to 5 MPa resulted in 89% porosity with partial interconnection between the pores in the polymeric matrix.

An in depth knowledge on how a polymer behaves in a gas medium at various conditions can serve as an important tool in designing processes whereby scaffolds with specific geometries and properties are created. Changes in the physical properties of a polymer can have an effect on the porous morphologies generated. Consequently, changes induced by the gas are an important factor to be considered when designing porous structures for specific applications. Depending on the gas saturation conditions, favorable interaction between the polymer and gas, as well as the thermodynamic instability induced, morphologies with various void sizes can be obtained.[10,11] CO_2 gas is known to swell and significantly plasticize many amorphous polymers and in some cases to induce crystallinity.[12−16] Absorbed CO_2 reduces the polymer's glass-transition temperature (T_g) due to an increase in the free-volume fraction. Higher gas solubility in the polymer results in further relaxation and mobility of the polymer chains and hence a drastic reduction in polymer's T_g and the possibility of transition from glassy to rubbery state. Conditioning semicrystalline polymers with CO_2 can result in a reduction of the cold-crystallization temperature and hence possible foaming difficulties while processing the samples.[17−19] Furthermore, crystalline polymers typically dissolve a smaller amount of gas than an amorphous polymer due to the lower amorphous volume fraction available in the sample.[20]

The porous matrices generated from amorphous polymers by CO_2 are normally uniform due to the homogeneous nucleation. Other factors that affect the size and distribution of pores in amorphous polymers are solubility of the gas in the polymer and its subsequent rate of diffusion out of the matrix.[10] In semicrystalline polymers, the absorption and diffusion of the gas almost exclusively occurs through the amorphous regions, resulting in a nonuniform dissolution of the gas which influences the resultant foam structure.[21−23] As such, a control on the rate of crystallization in polymers affects the type of porous morphology generated.[17]

Although there are many studies on the formation of foams with CO_2 gas in petrochemical based resins, little data is available on biodegradable polymers. Of the reported cases, limited investigations have been focused on the fundamentals of the biopolymer−gas interactions and the subsequent physical changes induced in the polymer. A detailed investigation on the fundamental interaction of CO_2 with poly (lactide acid) (PLA) in the temperature range 40−190 °C and pressures up to 10 MPa with subsequent gas induced crystallization was reported recently.[24,25] Although CO_2 induced crystallization in

* To whom correspondence should be addressed. Telephone: (613) 993-9698. Fax: (613) 991-2384. E-mail: Victoria.Nawaby@nrc-cnrc.gc.ca.
[†] Institute for Chemical Process and Environmental Technology.
[‡] Industrial Materials Institute.

10.1021/bm060738u CCC: $33.50 Published 2006 by the American Chemical Society
Published on Web 10/18/2006

PLA is observed at supercritical conditions, its effect at subcritical conditions is not reported. This paper therefore demonstrates a single step solvent free method at sub-critical conditions able to generate various types of poly(L-lactic acid) (PLLA) morphologies with potential biomedical applications.

Experimental Section

Material. The biobased polymer PLA is synthesized via ring opening polymerization of lactide and due to its chiral nature it is divided into L and D enantionmers.[26] Control on the L to D ratio in the monomer content is an important molecular feature which has a large effect on crystallization of PLA and its properties. Greater stereochemical purity in this polymer (i.e., a higher L content) favors crystallization.[27] Commercially, amorphous poly (D,L-lactic acid) (PDLLA), semicrystalline PLLA, as well as D-PLA and L-PLA copolymer known as PLA are available. PLLA pellets (lot # D02052, $M_w = 58\,000$ and $M_w/M_n = 1.7$) with density of 1.24 g/cm^3, $T_g = 54$ °C, $T_c = 83$ °C, and $T_m = 170$ °C were supplied by Birmingham Polymer Inc. Bonedry 99% pure CO_2 was used.

Gas Solubility Measurements. PLLA sheets 400 μm thick were prepared by compression molding at 190 °C followed by quenching in ice water. CO_2 sorption kinetic studies were carried out using a CAHN D110 microbalance. The detailed description of this gravimetric technique has been reported elsewhere.[28] A polymer sample (0.3 g) was loaded in the balance, and the system was evacuated for 48 h prior to pressurizing to the desired value at 25 °C. The changes in the polymer mass as a result of gas uptake were recorded as a function of time (every 10 s) and a period of 24 h was required for the system to reach equilibrium. The system was then pressurized to the next value at a rate of 0.034 MPa per minute by introducing an additional amount of gas into the balance. This was continued until measurements over the desired pressure range were completed. Blank runs under the same experimental conditions provided the balance zero-shift as a function of pressure, and equilibrium mass readings were corrected for the zero-shift. Buoyancy corrections were also applied to the solubility data since a small volume difference between the sample and reference side in the balance develops as a result of matrix dilation. Diffusion coefficients of the gas in the polymer were subsequently derived from the corrected sorption kinetic data.[28]

CO_2 Induced Crystallization. A Bruker GADDS diffraction system using Co Kα and a 2D HISTAR detector was used to analyze the compression-molded samples. The CO_2 untreated samples as examined by XRD data were amorphous, and the effect of CO_2 on PLLA was investigated by treating the polymer with different gas pressures and contact times. Polymer sheets were subsequently saturated with CO_2 at 25 °C and various pressures for different time intervals. The pressure in the saturation vessel was released rapidly, and samples were aged for at least 5 days prior to obtaining X-ray diffraction patterns. The samples were analyzed in transmission mode with a 1 mm monocapillary optic and a collimator-mounted beamstop. The background scatter was subtracted from the collected frames after accounting for the attenuation of the scattering by the sample using $I/I_0 = te^{(-\mu t)}$, where t is the sample thickness and μ is the linear absorption coefficient. The background-corrected frames were then analyzed using the rolling-ball algorithm in the Bruker GADDS software to separate the crystalline and amorphous fractions. The physical changes induced in the polymer after treatment with CO_2 were also studied using differential scanning calorimetry (DSC 2920, TA instruments Inc) and subsequently compared to the untreated samples. The heating rate was set at 10 °C/min, and samples were heated from room temperature up to 190 °C under a nitrogen (N_2) environment set at a flow rate of 50 mL/min.

Foaming and Foam Characterization. Foamed specimens were prepared by saturating PLLA samples with CO_2 at 25 °C and various pressures and saturation times. The samples were then foamed in the temperature range 50−100 °C and foam morphologies were analyzed using Hitachi field emission scanning electron microscopy (S4800) at 2.0 kV and 10 μA current.

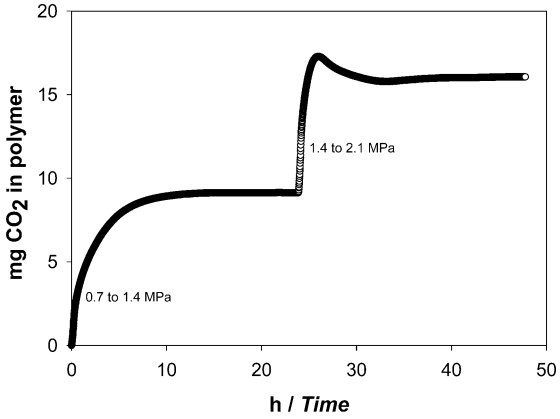

Figure 1. Sorption kinetics of CO_2 in PLLA at 25 °C for two pressure jumps, 0.7 to 1.4 MPa and then from 1.4 to 2.1 MPa.

Table 1. Pressure Dependence of CO_2-Induced Crystallization at 25 °C for 24 h

pressure, MPa	2.1	2.8	3.4	4.1	5.5
crystallinity, %	13.1	16.0	20.8	23.4	23.6

Results and Discussion

In this study, the solubility of CO_2 in PLLA at 25 °C as a function of pressure was investigated. The sorption curves below 1.4 MPa reached a maximum value and no further mass changes were observed once the system had reached equilibrium. However, with an increase in pressure above 1.4 MPa, the sorption curves exhibit a characteristic knee indicating the polymer being crystallized in the presence of CO_2 (Figure 1). This observed decrease in solubility is due to the formation of crystal domains in the polymer and hence rejection of gas from the polymer−CO_2 solution. This gas-induced crystallization observed in the PLLA−CO_2 system resembles the behavior previously observed in the poly(ethylene terephthalate) (PET)−CO_2 system.[18,19]

Since the dissolution of CO_2 in PLLA induces physical changes in the matrix, the properties of the resulting material were evaluated using thermal analysis and X-ray diffraction studies. The % crystallinity in the samples as a function of gas pressure was determined, and values of the gas-induced crystallinity for pressures above 2 MPa are presented in Table 1.

In the case of semicrytalline polymers, the crystal domains do not contribute to the gas uptake; hence, the sorption of gas only occurs in the amorphous fraction. Consequently, the equilibrium solubility data and diffusion coefficients of the gas in PLLA at pressures above 2 MPa were corrected, and values in the amorphous fraction are presented. The overall equilibrium sorption curve as a function of pressure was linear and followed Henrian behavior. The determined Henry's law constant (k_H) value for PLLA−CO_2 system at 25 °C was 52.08 mg/g PLLA*MPa. The amount of gas uptaken at 5.5 MPa in the amorphous fraction of PLLA is about 300 mg/g of polymer. This value is higher than solubility of CO_2 in poly(methyl methacrylate) (PMMA) under the same experimental condition (230 mg/g of polymer).[10] The high CO_2 solubility in PMMA as compared to, for example, polystyrene (PS) is reported to be due to the strong interaction between CO_2 and the electron-donating functional (carbonyl) groups in PMMA. The intermolecular interaction of CO_2 with PMMA suggest this type of

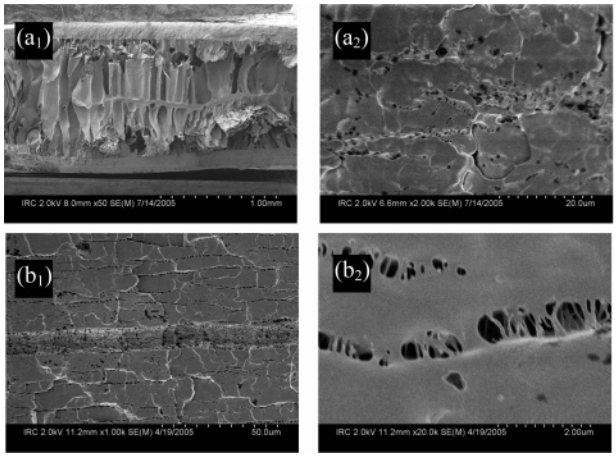

Figure 2. SEM microphotographs of PLLA foams as a function of saturation time at 25 °C, 5.5 MPa, and foamed at 60 °C. (a_1) 5 min, ×100; (a_2) 5 min, skin ×2000; (b_1) 24 h, ×1000; (b_2) 24 h, ×20 000.

Table 2. Time Dependence of CO_2-Induced Crystallization at 25 °C and 5.5 MPa

time	3 min	5 min	7 min	10 min	24 h
crystallinity, %	15.6	21.5	22.5	23.2	23.6

interaction is possible between CO_2 and other polymers containing Lewis base groups.[29,30] Therefore, the high solubility of CO_2 in PLLA is thought to be due to the specific interactions of gas with the carbonyl groups in PLLA.

The diffusion coefficients of CO_2 at various pressures were determined by fitting the sorption kinetic data to a hybrid model that combines both short and long-term Fickian diffusion equations.[28] The obtained values of diffusion coefficient range from 5.5×10^{-9} to 1.4×10^{-7} cm^2/s in the tested pressure range 0.34−5.5 MPa. In systems whereby the solubility of the gas in the polymer is high, the diffusion coefficient as a function of pressure exhibits a concentration dependent behavior, and hence a sharp increase in diffusion coefficient is observed indicating a transition from glassy to the rubbery state in the polymer. Extensive plasticization of polymers by gas as reported previously in PMMA, acrylonitrile−butadiene−styrene (ABS), and syndiotactic poly(methyl methacrylate) (sPMMA)−CO_2 systems resulted in a distinctive increase in the diffusion coefficient curves.[10,31] The pressure at which this change occurs is defined as the glass transition pressure (p_g); in the PLLA−CO_2 system, a sharp increase was observed at about 1.6 MPa.

Formation of porous morphologies in PLLA using CO_2 as the blowing agent was investigated at 25 °C by varying the gas pressure, contact time and foaming temperature. The samples contacted with CO_2 for 24 h and pressures in the range 2.1 to 5.5 MPa resulted in an increase in pore density with an increase in pressure up to 4.1 MPa at 90 °C. Due to CO_2 induced crystallization in the polymer and an increase in matrix stiffness, above 4.1 MPa foaming difficulties were encountered, and specimens were regionally foamed. The foam morphology however in the tested pressure range (2.1−5.5 MPa) resulted in partially interconnected pores in the foaming temperature range 60−100 °C.

Foaming of crystalline polymers is relatively difficult as compared to amorphous polymers due to regional dissolution of CO_2 gas in the polymer. In amorphous polymers with an increase in pressure, an influence on pore nucleation and pore density is observed through two dominant factors: a decrease in the free energy barrier for formation of stable nuclei and the activation of additional nucleating sites due to swelling and changes in the free volume of the matrix.[18] However, induced crystallinity in polymers by CO_2 is an additional effect on the foam morphology as observed in PET−CO_2 systems.[17]

To further investigate the possible effect of crystallites on the formation of porous morphologies in PLLA upon treatment with CO_2, the role of treatment time was investigated. Since maximum crystallinity in samples was observed when treated with CO_2 at 25 °C and 5.5 MPa, the pressure was thus held constant and exposure time to CO_2 and foaming temperatures

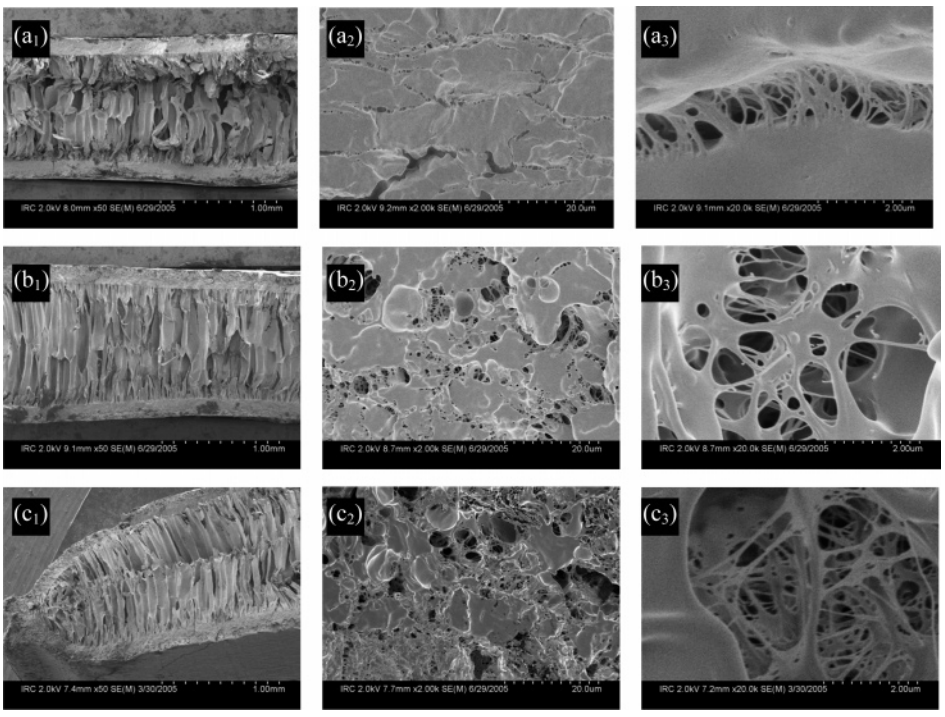

Figure 3. SEM microphotographs of CO_2-foamed PLLA samples saturated at 25 °C and 5.5 MPa for 5 min and foamed at (a_1) 70 °C, ×50; (a_2) 70 °C, skin ×2000; (a_3) 70 °C, skin ×20 000; (b_1) 80 °C, ×50; (b_2) 80 °C, skin ×2000; (b_3) 80 °C, skin ×20 000; (c_1) 90 °C, ×50; (c_2) 90 °C, skin ×2000; (c_3) 90 °C, skin ×20 000.

were varied. The effect of contact time is demonstrated with the changes in the crystalline content obtained (Table 2).

A skin-core structure was observed in samples treated for 3 and 5 min. This is consistent with the sorption kinetic data which indicated with shorter contact times a limited degree of gas diffusion occurs in the sample. Therefore, the interior (core) part of the sample remains amorphous thereby facilitating the formation of two distinctive porous regions upon foaming (Figure 2, panels a_1 and a_2). The short contact time allows for part of the sample to crystallize upon contact with CO_2 and the porous structure obtained in the core to be significantly different in terms of pore size and texture. As a result of a lower degree of gas solubility with a shorter contact time, a higher rate of gas diffusion out of the amorphous region occurs due to a lower degree of matrix stiffness, and hence, pores obtained in the core are large and stretched. With an increase in contact time above 5 min, a higher degree of crystallinity in the sample occurred and the skin−core structure completely disappeared. Meanwhile, samples contacted with CO_2 for 24 h produced fine-layered interconnected morphologies with partially open pores in the size range 200−500 nm within the layer (Figure 2, panels b_1 and b_2). The mechanism by which the layered structure in the PLLA matrix occurs is not yet fully understood; however, it is thought to be due to nucleation occurring at the lower energy barrier regions at the amorphous/crystalline boundaries and possible microvoids within the matrix.

The skin−core was most evident for samples treated for 5 min with 5.5 MPa of CO_2 at 25 °C and subsequently foamed at different temperatures (Figure 3). Unlike the typical polymer foam structure obtained with CO_2 where it consists of a porous core and a nonporous skin, PLLA foam shows stretched pores in the core (Figure 3, panels a_1, b_1, and c_1) and partial interconnected pores in the skin (Figure 3, panels a_2, b_2, and c_2). The formation of a nonporous skin in the foaming process as described in the literature can be attributed to a rapid outward diffusion of gas molecules near the edges of the sample than joining nuclei.[32] This rapid diffusion of gas out of the sample creates a depletion layer near the edges in which the gas concentration is too low to significantly contribute to nucleation and pore growth. Hence, the morphologies generated can be attributed to the high degree of solubility of CO_2 in PLLA, which provides enough gas for pore nucleation and growth in the skin. With an increase in foaming temperature from 70 to 90 °C, further pore nucleation in the skin occurred and a significant improvement on pore interconnection and degree of openness was observed (Figure 3, panels a_3, b_3, and c_3).

Specimens foamed at 70 °C resulted in the core of the samples to have elongated pores (Figure $3a_1$), with a skin comprising of layered open pore structure (Figure 3, panels a_2 and a_3). With an increase in temperature to 80 °C, the pore elongation in the core of the samples became more defined in addition to obtaining a higher degree of open interconnected pores in the skin (Figure 3, panels b_1, b_2, b_3). The pore size in the core is in the range of 50−100 μm and found to be in the range of 0.2−2 μm in the skin (Figure 3, panels b_1 and b_3). A further increase to 90 °C resulted in a less uniform porous morphology in the core (Figure $3a_1$); however, a higher number of smaller pore sizes were nucleated in the skin at this temperature (Figure 3, panels c_2 and c_3).

CO_2-induced crystallinity in PET has been reported to be the dominant factor affecting nucleation and growth in the microporous foams obtained, and crystallized PET shows small pore sizes and large pore densities. CO_2-induced crystallization was found to play a major role in morphological modifications in this system.[17] Therefore, in light of the current findings on PLLA−CO_2 systems at subcritical conditions, a detailed investigation on the role of crystallinity on foam morphologies is being carried out and is being presented in a forthcoming paper.

To date, most scaffolds generated for tissue engineering applications are by means of a solvent based process or a high-temperature technique which often involves multiple steps. Control on pore size and degree of porosity is yet another factor to be considered when fabricating scaffolds. This paper demonstrates that by simple changes in CO_2 processing parameters polymer foams with intriguing morphologies and a characteristic skin−core structure can be generated. Different pore shapes and sizes in the core as well as open and interconnected pores within the skin were obtained with small changes in the processing conditions. The core of the generated scaffolds consists of larger pores ideal for cell growth, and the skin with open and interconnected smaller pores is thought to be ideal as a passageway for the flow of nutrients. Hence, the resultant morphologies presented in this study can have potential applications in the biomedical field.

Acknowledgment. The authors thank Mr. James Margeson for his assistance with SEM work.

References and Notes

(1) Harley, B. A.; Hastings, A. Z.; Yannas, I. V.; Sannino, A. *Biomaterials* **2006**, *27*, 866.
(2) Singh, L.; Kumar, V.; Ratner, B. D. *Biomaterials* **2004**, *25*, 2611.
(3) Moore, J. M.; Friedman, J. A.; Lewellyn, E. B.; Mantila, S. M.; Krych, A. J.; Ameenuddin, S.; Knight, A. M.; Lu, L.; Currier, B. L.; Spinner, R. J.; Marsh, R. W.; Windebank, A. J.; Yaszemski, M. J. *Biomaterials* **2006**, *27*, 419.
(4) Harris, L. D.; Kim, B. S.; Mooney, D. J. *J. Biomed. Mater. Res.* **1998**, *42*, 396.
(5) Whang, K.; Thomas, C. H.; Healy, K. E.; Nuber, G. A. *Polymer* **1995**, *36*, 837.
(6) Lo, H.; Kadiyala, S.; Guggino, E.; Leong, K. W. *J. Biomed. Mater. Res.* **1996**, *30*, 475.
(7) Schugens, Ch.; Maquet, V.; Grandfils, C.; Jerome, R.; Teyssie, Ph. *Polymer* **1996**, *37*, 1027.
(8) Freed, L. E.; Vunjak-Novakovic, G.; Biron, R. J.; Eagles, D. B.; Lesnoy, D. C.; Barlow, S. K.; Langer, R. *Bio/Technology* **1994**, *12*, 689.
(9) Park, A.; Wu, B.; Griffith, L. G. *J. Biomater Sci. Polym. Ed.* **1998**, *9*, 89.
(10) Handa, Y. P.; Zhang, Z.; Wong, B. *Cell. Polym.* **2001**, *20*, 1.
(11) Goel, S. K.; Beckman, E. J. *Polym. Eng. Sci.* **1994**, *34*, 1137.
(12) Hanada, Y. P.; Roovers, J.; Wang, F. *Macromolecules* **1994**, *27*, 5511.
(13) Beckman, E.; Porter, R. S. *J. Polym. Sci. Polym. Phys.* **1987**, *25*, 1511.
(14) Schultze, J. D.; Engelman, I. A. D.; Boehning, M.; Springer, J. *Polym. Adv. Technol.* **1991**, *2*, 123.
(15) Handa, Y. P.; Zhang, Z.; Wong, B. *Macromolecules* **1997**, *30*, 8499.
(16) Handa, Y. P.; Zhang, Z.; Roovers, J. *J. Polym. Sci. Polym. Phys.* **2001**, *39*, 1505.
(17) Baldwin, D. F.; Shimbo, M.; Suh, N. P. *J. Eng. Mater. Technol.* **1995**, *117*, 62.
(18) Baldwin, D. F.; Park, C. B.; Suh, N. P. *Polym. Eng. Sci.* **1996**, *36*, 1437.
(19) Baldwin, D. F.; Park, C. B.; Suh, N. P. *Polym. Eng. Sci.* **1996**, *36*, 1446.
(20) Chen, D.; Hsue, G. *Polymer* **1993**, *35*, 2808.
(21) Handa, Y. P.; Zhang, Z.; Nawaby, V.; Tan, J. *Cell. Polym.* **2001**, *20*, 241.
(22) Sha, H.; Harrison, I. R. *J. Polym. Sci. Polym. Phys.* **1992**, *30*, 915.
(23) Doroudiani, S.; Park, C. B.; Kortschot, M. T. *Polym. Eng. Sci.* **1996**, *36*, 2645.
(24) Sato, Y.; Yamane, M.; Sorakubo, A.; Takishima, S.; Masuoka, H.; Yamamoto, H.; Takasugi, M. *Jpn. Symp. Thermophys. Prop.* **2000**, *B231*, 196.
(25) Takada, M.; Hasegawa, S.; Ohshima, M. *Polym. Eng. Sci.* **2004**, *44*, 186.
(26) Kricheldorf, H. R.; Berl, M.; Scharngal, N. *Macromolecules* **1988**, *21*, 286.

(27) Lehermeier, H. J.; Dorgan, J. R.; Way, J. D. *J. Membrane Sci.* **2001**, *190*, 243.
(28) Wong, B.; Zhang, Z.; Handa, Y. P. *J. Polym. Sci. Polym. Phy.* **1998**, *36*, 2025.
(29) Kazarian, S. G.; Vicent, M. F.; Bright, F. V.; Liotta, C. L.; Eckert, C. A. *J. Am. Chem. Soc.* **1996**, *118*, 1729.
(30) Kazarian, S. G. *Macromol. Symp.* **2002**, *184*, 215.
(31) Nawaby, A. V.; Handa, Y. P.; Liao, X.; Yamamoto, Y.; Mizumoto, T. *Polym. Int.* **2006**, in press.
(32) Kumar, V.; Wells, J. E. *SPE ANTEC Technol. Pap.* **1992**, *38*, 1508.

BM060738U